Journal of Sound and Vibration 391 (2017) 1–19

Contents lists available at ScienceDirect

Journal of Sound and Vibration

journal homepage: www.elsevier.com/locate/jsvi

On spatial spillover in feedforward and feedback noise control

Antai Xie, Dennis Bernstein *

Department of Aerospace Engineering, University of Michigan, 1320 Beal Ave., Ann Arbor, MI 48109, USA

ARTICLE INFO

Article history:
Received 29 April 2016
Received in revised form
27 October 2016
Accepted 1 December 2016
Handling Editor: A.V. Metrikine
Available online 10 December 2016

Keywords:
Spatial spillover
Feedback noise control
Feedforward noise control
Transmissibility

ABSTRACT

Active feedback noise control for rejecting broadband disturbances must contend with the Bode integral constraint, which implies that suppression over some frequency range gives rise to amplification over another range at the performance microphone. This is called *spectral spillover*. The present paper deals with *spatial spillover*, which refers to the amplification of noise at locations where no microphone is located. A spatial spillover function is defined, which is valid for both feedforward and feedback control with scalar and vector control inputs. This function is numerically analyzed and measured experimentally. Obstructions are introduced in the acoustic space to investigate their effect on spatial spillover.

1. Introduction

Active noise suppression has been extensively studied for several decades, and numerous techniques have been developed, analyzed, and tested, with several highly successful applications [1–3]. Noise suppression algorithms can be classified as either feedforward or feedback. Feedforward algorithms assume that a direct or indirect measurement of the disturbance is available, and this signal is passed through an adaptive filter to a control speaker [2,3]. These algorithms assume that the disturbance measurement is not corrupted by the control-speaker output, which means that the transfer function from the control input to the disturbance measurement is zero.

In some applications, however, it is difficult to measure the disturbance. For example, it is difficult for external sensors to measure the effect of broadband road and wind noise on the interior of the vehicle. If internal microphones are used, then the measurements include the effect of the control speakers. In this situation, feedback control is more appropriate than feedforward control. However, feedback control is susceptible to instability in the event of model errors.

Furthermore, although feedback control can suppress broadband noise, the Bode integral constraint implies that reducing the magnitude of the frequency response at the performance microphone is impossible at all frequencies [4–6]. For narrowband disturbances, this does not present a problem since the noise spectrum is confined to a limited bandwidth. However, for broadband disturbances, it is inevitable that, at least in some frequency range, the closed-loop noise level is amplified relative to the open-loop noise level. The challenge is thus to shape the closed-loop response so that *spectral spillover* has minimal effect on the closed-loop performance.

Beyond spectral spillover, yet another challenge is *spatial spillover*. Spatial spillover refers to the phenomenon where a controller may suppress noise at one location (the location of the performance microphone) but amplify it at another location (the location of an evaluation microphone). Due to restrictions in the design of a system, a performance

* Corresponding author.
E-mail address: dsbaero@umich.edu (D. Bernstein).

http://dx.doi.org/10.1016/j.jsv.2016.12.002
0022-460X/

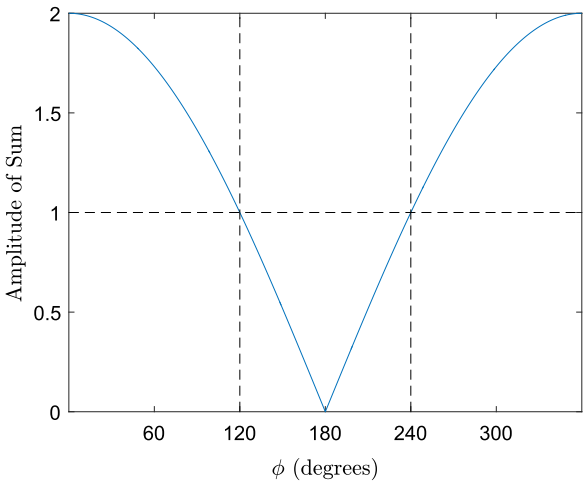

Fig. 1. Amplitude of the sum of two unit-amplitude sinusoids with identical frequency ω and relative phase ϕ. For $\phi = 180°$, perfect cancellation occurs, and thus, the amplitude of the sum is zero. For $\phi = 180 \pm 60°$, the amplitude of the sum is 1. The plot is based on the fact that $\sin(\omega t) + \sin(\omega t + \phi) = 2\cos(\phi/2)\sin(\omega t + \phi/2)$.

microphone may not always be placeable at all locations in which it is desirable to suppress noise. Thus, in the design phase, it is crucial to understand the relation between where the performance microphone is placed and evaluation locations where it is desirable to suppress noise.

The notion of spatial spillover defined in this paper concerns the decrease in the noise amplitude at the location of the performance microphone relative to its open-loop level as compared to the decrease in noise amplitude at the location of the evaluation microphone relative to its open-loop level. Consequently, spatial spillover is a measure of the relative effectiveness of the control at different locations. This notion is distinct from the fact, as shown in Fig. 1, that the sum of two unit-amplitude sinusoidal waves of the same frequency may possess any amplitude between 0 and 2 depending on the relative phase shift of the waves. Consequently, a disturbance sinusoid and a control-speaker sinusoid may add destructively at one location and constructively at another location depending on the phase shift between the waves at these locations. This notion is often used to estimate the bandwidth in which control is effective within an acoustic space. However, this phenomenon per se says nothing about the relationship between open- and closed-loop noise levels at a given location, and thus is not relevant to spatial spillover as defined and analyzed in this paper.

The goal of the present paper is to investigate the phenomenon of spatial spillover within a 3D acoustic space. To do this, we define a spatial spillover function for both feedforward and feedback control. It turns out that the spatial spillover function has the same functional form for both feedforward and feedback control and, in addition, is independent of the control in the case of scalar control. We also show that the spatial spillover function can be expressed as a ratio of transmissibility functions.

For illustrative 2DOF models, we consider feedforward and feedback controllers and compute the spatial spillover function. We then implement feedforward and feedback controllers in a series of noise control experiments with broadband disturbances. We measure the response at the locations of the performance and evaluation microphones, and we use this data to experimentally determine the spatial spillover function.

In certain applications, obstructions that are difficult to model may be present in the acoustic space, for example, passengers in a vehicle. We thus introduce obstructions between the performance and evaluation microphones in order to determine the effect on the spatial spillover function. The experimental results show that the presence of an obstruction can shift the magnitude and phase of the spatial spillover function relative to the acoustic space without the obstruction. A preliminary version of some of the results in this paper appeared in [7].

The contents of the paper are as follows. In Section 2, the spatial spillover function for feedforward control is derived, and numerical examples are presented in Section 3. In Section 4, the spatial spillover function for feedback control is derived, and numerical examples are presented in Section 5. Section 6 expresses the spatial spillover function in terms of transmissibility functions. Experimental results are presented in Section 7, and conclusions are discussed in Section 8.

2. Spatial spillover function for feedforward control

Consider the feedforward control problem shown in Fig. 2, where $z \in \mathbb{R}$ is the performance variable, $e \in \mathbb{R}$ is the evaluation variable, $w \in \mathbb{R}$ is the disturbance, and $u \in \mathbb{R}^{l_u}$ is the control input. Note that z, e, and w are scalar signals and that u may be either a scalar or vector signal depending on whether $l_u = 1$ or $l_u > 1$, respectively. The dynamics and signals may be either continuous time or discrete time.

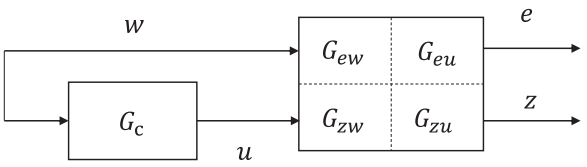

Fig. 2. Feedforward control.

It follows from Fig. 2 that

$$z = G_{zu}u + G_{zw}w, \tag{1}$$

$$e = G_{eu}u + G_{ew}w, \tag{2}$$

where the feedforward control u is given by

$$u = G_c w. \tag{3}$$

Therefore,

$$z = \widetilde{G}_{zw}w, \tag{4}$$

$$e = \widetilde{G}_{ew}w, \tag{5}$$

where

$$\widetilde{G}_{zw} \triangleq G_{zu}G_c + G_{zw}, \tag{6}$$

$$\widetilde{G}_{ew} \triangleq G_{eu}G_c + G_{ew}. \tag{7}$$

Define the *spatial spillover function* G_{ss} by

$$G_{ss} \triangleq \frac{\dfrac{\widetilde{G}_{ew}}{G_{ew}} - 1}{\dfrac{\widetilde{G}_{zw}}{G_{zw}} - 1}. \tag{8}$$

Note that, if $G_{zu}G_c = 0$, then $\widetilde{G}_{zw} = G_{zw}$, and thus the spatial spillover function is undefined. We therefore assume that $G_{zu}G_c \neq 0$. G_{ss} relates the performance of the controlled system relative to the uncontrolled system at e to the performance of the controlled system relative to the uncontrolled system at z. It follows from (6) and (7) that

$$\frac{\widetilde{G}_{zw}}{G_{zw}} - 1 = \frac{G_{zu}G_c}{G_{zw}}, \tag{9}$$

$$\frac{\widetilde{G}_{ew}}{G_{ew}} - 1 = \frac{G_{eu}G_c}{G_{ew}}, \tag{10}$$

and thus (8)–(10) implies that

$$G_{ss} = \frac{G_{eu}G_cG_{zw}}{G_{zu}G_cG_{ew}}. \tag{11}$$

In the case where u is scalar, that is, $l_u = 1$, it follows that

$$G_{ss} = \frac{G_{eu}G_{zw}}{G_{zu}G_{ew}}, \tag{12}$$

which is independent of G_c. Note that G_{ss} is a rational function of the Laplace or Z-transform variable. However, G_{ss} is not a transfer function since it may be improper and does not have input and output signals that can be specified in terms of z, e, w, and u.

3. Feedforward control numerical examples

Consider a discrete-time state-space representation of (1), (2) given by

$$x(k+1) = Ax(k) + Bu(k) + D_1 w(k), \tag{13}$$

$$z(k) = E_1 x(k), \tag{14}$$

$$e(k) = Cx(k), \tag{15}$$

where

$$G_{zw}(\mathbf{z}) = E_1(\mathbf{z}I - A)^{-1}D_1, \tag{16}$$

$$G_{zu}(\mathbf{z}) = E_1(\mathbf{z}I - A)^{-1}B, \tag{17}$$

$$G_{ew}(\mathbf{z}) = C(\mathbf{z}I - A)^{-1}D_1, \tag{18}$$

$$G_{eu}(\mathbf{z}) = C(\mathbf{z}I - A)^{-1}B, \tag{19}$$

and the state-space representation of the feedforward controller (3) given by

$$x_c(k+1) = A_c x_c(k) + B_c w(k), \tag{20}$$

$$u(k) = C_c x_c(k) + D_c w(k), \tag{21}$$

where

$$G_c(\mathbf{z}) = C_c(\mathbf{z}I - A_c)^{-1}B_c + D_c,$$
$$x_c \in \mathbb{R}^{n_c}. \tag{22}$$

In the subsequent feedforward numerical examples, the discrete-time state-space systems are chosen arbitrarily as a 4th-order system with two modes. We assume that w is zero-mean Gaussian white noise with standard deviation 1. Feedforward controllers are designed to suppress the effect of w at z. No considerations are made in the controller design to suppress the effect of w at e. The details of the controller design are omitted since they are not relevant to the analysis.

In each example we compare the spatial spillover function for two different feedforward controller designs applied to the same system. The spatial spillover function is computed using (8) which is a function of G_{zw}, G_{ew}, $\widetilde{G}_{zw}$ given by (6), and $\widetilde{G}_{ew}$ given by (7). We demonstrate that, if $l_u = 1$, then (8) is independent of G_c, whereas if $l_u > 1$, then (8) is not independent of G_c.

Example 1. G_{ss} for feedforward control with scalar control u. Consider the 4th-order system

$$A = \begin{bmatrix} 0.45 & 1 & 0 & 0 \\ -0.05 & 0.45 & -0.37 & -0.66 \\ 0 & 0 & 0.38 & 1 \\ 0 & 0 & -0.76 & 0.38 \end{bmatrix}, \quad B = \begin{bmatrix} 0 \\ 1.01 \\ 0 \\ 0.76 \end{bmatrix}, \quad D_1 = \begin{bmatrix} -1.53 \\ 0 \\ -1.11 \\ -1.04 \end{bmatrix}, \tag{23}$$

$$E_1 = \begin{bmatrix} -0.15 & 0.99 & 0 & 0 \end{bmatrix}, \quad C = \begin{bmatrix} 0.99 & 0.26 & -0.38 & 0.17 \end{bmatrix}. \tag{24}$$

Assuming that this discrete-time model arises from sampling a continuous-time system at the sample rate of 1 kHz, the corresponding continuous-time modal frequencies are $\omega_{n1} = 132$ Hz and $\omega_{n2} = 185$ Hz with damping ratios $\zeta_1 = 0.831$ and $\zeta_2 = 0.043$, respectively. We apply two different feedforward controllers to this system, namely,

$$A_c = \begin{bmatrix} 0.52 & 0.74 & 0 \\ -0.74 & 0.52 & 0 \\ 0 & 0 & -0.30 \end{bmatrix}, \quad B_c = \begin{bmatrix} -0.70 \\ -1.14 \\ 0.49 \end{bmatrix}, \tag{25}$$

$$C_c = \begin{bmatrix} 0.59 & -0.23 & -0.17 \end{bmatrix}, \quad D_c = -0.12 \tag{26}$$

and

$$A_c = \begin{bmatrix} 0.62 & 0.67 & 0 & 0 \\ -0.67 & 0.62 & 0 & 0 \\ 0 & 0 & -0.54 & 0 \\ 0 & 0 & 0 & -0.01 \end{bmatrix}, \quad B_c = \begin{bmatrix} 1.39 \\ 2.15 \\ -0.94 \\ 0.56 \end{bmatrix}, \tag{27}$$

$$C_c = \begin{bmatrix} -0.56 & 0.18 & 0.15 & 0.21 \end{bmatrix}, \quad D_c = -0.18. \tag{28}$$

For both controllers, Fig. 3 shows the frequency response of the controlled and uncontrolled system at z and e as well as the

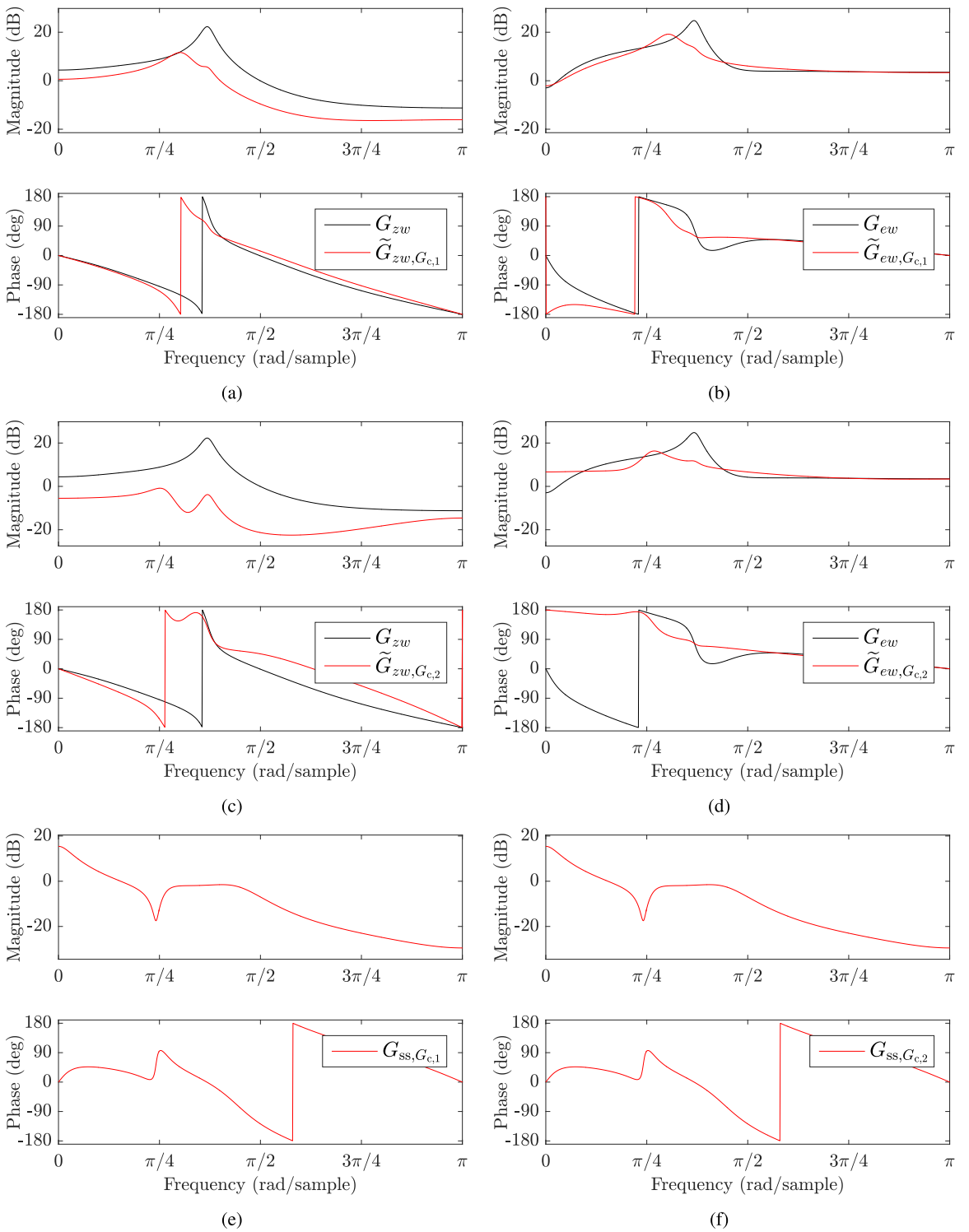

Fig. 3. Example 1: comparison of G_{ss} computed as (8) for feedforward control with scalar control u. (a) and (b) show the controlled and uncontrolled frequency response of the system (23), (24) using the controller (25), (26) denoted in the above legend as $G_{c,1}$; (c) and (d) show the controlled and uncontrolled frequency response of the system (23), (24) using the controller (27), (28) denoted in the above legend as $G_{c,2}$. Note that, since u is scalar, G_{ss} is independent of G_c, and thus (e), which shows the frequency response of G_{ss} for the controller (25), (26), is identical to (f), which shows the frequency response of G_{ss} for the controller (27), (28).

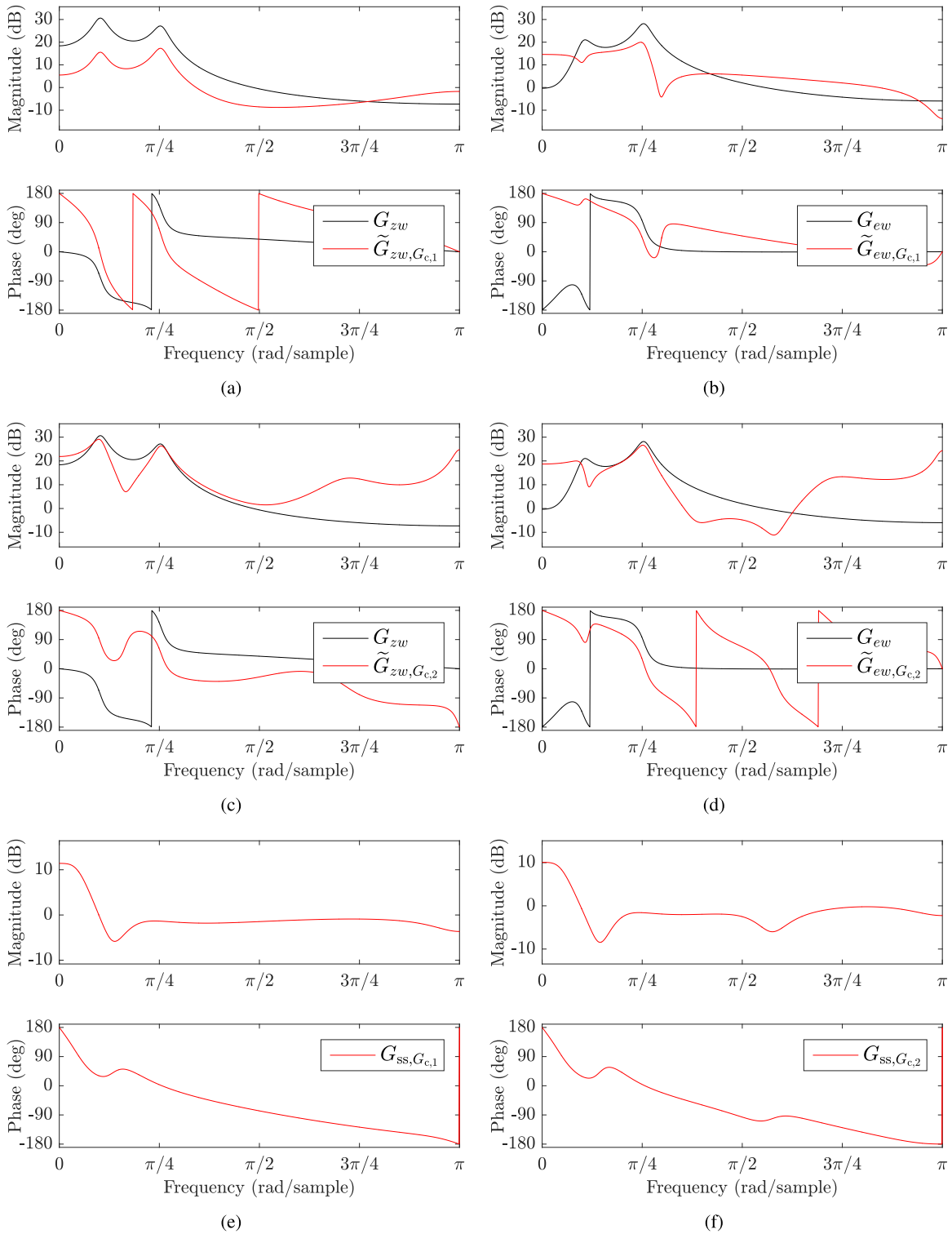

Fig. 4. Example 2: comparison of G_{ss} computed as (8) for feedforward control with vector control $u \in \mathbb{R}^2$. (a) and (b) show the controlled and uncontrolled frequency response of the system (29), (30) using the controller (31), (32) denoted in the above legend as $G_{c,1}$; (c) and (d) show the controlled and uncontrolled frequency response of the system (29), (30) using the controller (33), (34) denoted in the above legend as $G_{c,2}$. Note that, since u is a vector, G_{ss} depends on G_c, and thus (e), which shows the frequency response of G_{ss} for the controller (31), (32), differs from (f), which shows the frequency response of G_{ss} for the controller (33), (34).

frequency response of G_{ss}. Since u is scalar, G_{ss} is the same for both controllers.

Example 2. *G_{ss} for feedforward control with vector control $u \in \mathbb{R}^2$.* Consider the 4th-order system

$$A = \begin{bmatrix} 0.66 & 1 & 0 & 0 \\ -0.46 & 0.66 & 0.38 & 0.59 \\ 0 & 0 & 0.90 & 1 \\ 0 & 0 & -0.09 & 0.90 \end{bmatrix}, \quad B = \begin{bmatrix} 0 & 0 \\ 1.07 & 1 \\ 0 & 1 \\ 0.66 & 0 \end{bmatrix}, \quad D_1 = \begin{bmatrix} -0.57 \\ -0.31 \\ 0.27 \\ 1.33 \end{bmatrix}, \tag{29}$$

$$E_1 = \begin{bmatrix} 0.53 & 0.93 & 0 & 0 \end{bmatrix}, \quad C = \begin{bmatrix} 0.93 & 0.17 & -0.69 & -0.72 \end{bmatrix}. \tag{30}$$

Assuming that this discrete-time model arises from sampling a continuous-time system at the sample rate of 1 kHz, the corresponding continuous-time modal frequencies are $\omega_{n1} = 52$ Hz and $\omega_{n2} = 127$ Hz with damping ratios $\zeta_1 = 0.162$ and $\zeta_2 = 0.069$, respectively. We apply two different feedforward controllers to this system, namely,

$$A_c = \begin{bmatrix} -0.62 & 0 & 0 \\ 0 & 0.26 & 0.18 \\ 0 & -0.18 & 0.26 \end{bmatrix}, \quad B_c = \begin{bmatrix} -1.02 \\ -0.47 \\ -3.18 \end{bmatrix}, \tag{31}$$

$$C_c = \begin{bmatrix} -1.26 & 0.05 & 0.61 \\ 0.20 & 1.14 & -0.13 \end{bmatrix}, \quad D_c = \begin{bmatrix} 0.19 \\ 0.18 \end{bmatrix} \tag{32}$$

and

$$A_c = \begin{bmatrix} -0.95 & 0 & 0 & 0 \\ 0 & -0.51 & 0.64 & 0 \\ 0 & -0.64 & -0.51 & 0 \\ 0 & 0 & 0 & 0.33 \end{bmatrix}, \quad B_c = \begin{bmatrix} 4.22 \\ -1.16 \\ 3.16 \\ 0.86 \end{bmatrix}, \tag{33}$$

$$C_c = \begin{bmatrix} -0.75 & 0.74 & 0.20 & -1.89 \\ 0.14 & 0.28 & 0.19 & -1.77 \end{bmatrix}, \quad D_c = \begin{bmatrix} 0.29 \\ 0.27 \end{bmatrix}. \tag{34}$$

For both controllers, Fig. 4 shows the frequency response of the controlled and uncontrolled system at z and e as well as the frequency response of G_{ss}. Note that, since u is a vector, G_{ss} depends on G_c.

4. Spatial spillover function for feedback control

Consider the feedback control architecture shown in Fig. 5, where $z \in \mathbb{R}$ is the performance variable, $e \in \mathbb{R}$ is the evaluation variable, $w \in \mathbb{R}$ is the disturbance, and $u \in \mathbb{R}^{l_u}$ is the control input. The system may be either continuous time or discrete time.

It follows from Fig. 5 that

$$z = G_{zu}u + G_{zw}w, \tag{35}$$

$$e = G_{eu}u + G_{ew}w, \tag{36}$$

where the feedback control u is given by

$$u = G_c z. \tag{37}$$

Using (35) and (37) we obtain

$$z = \widetilde{G}_{zw}w, \tag{38}$$

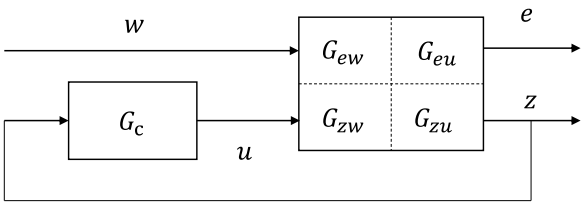

Fig. 5. Feedback control.

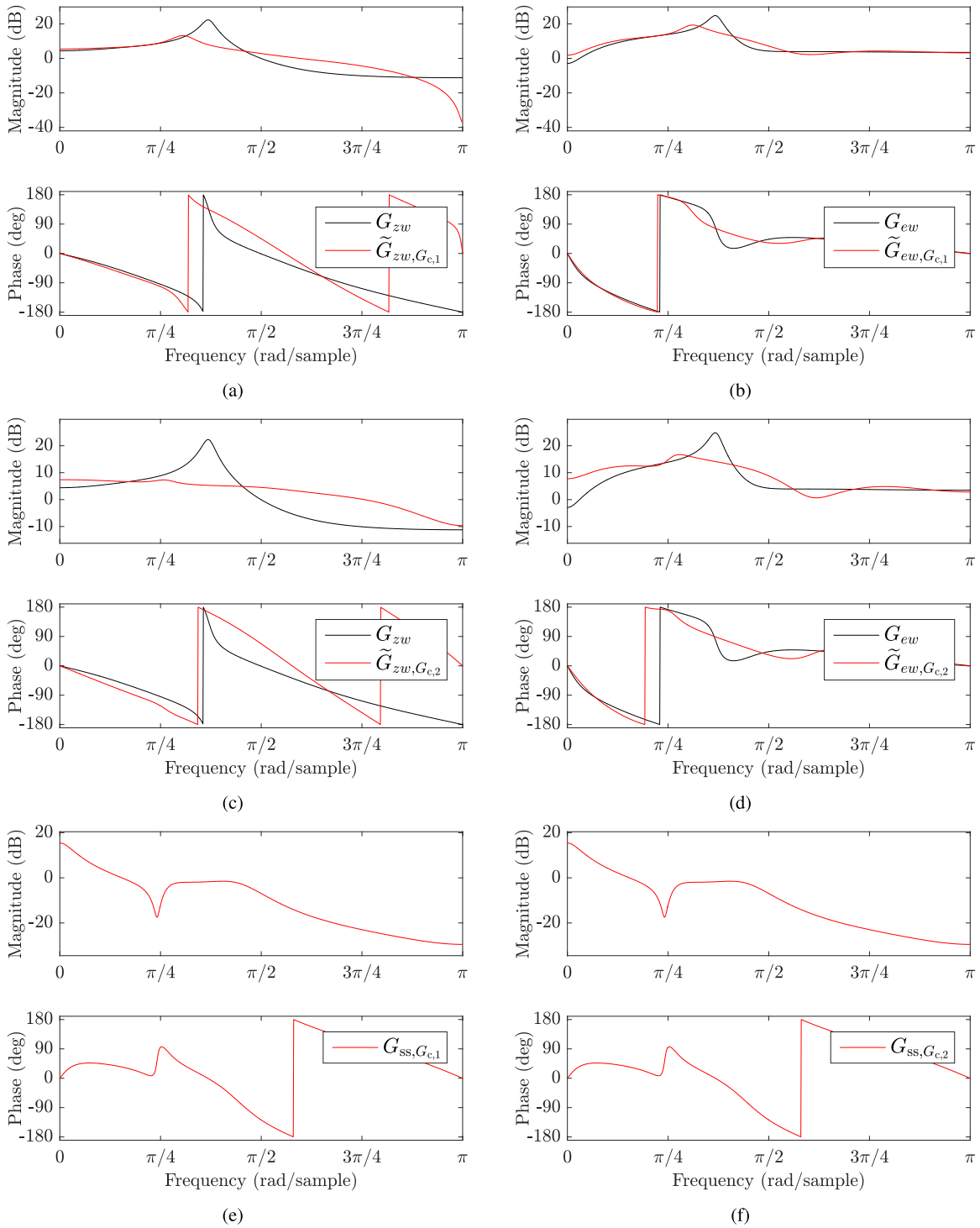

Fig. 6. Example 3: comparison of G_{ss} computed as (42) for feedback control with scalar control u. (a) and (b) show the controlled and uncontrolled frequency response of the system (23), (24) using the controller (50), (51) denoted in the above legend as $G_{c,1}$; (c) and (d) show the controlled and uncontrolled frequency response of the system (23), (24) using the controller (52), (53) denoted in the above legend as $G_{c,2}$. Note that, since u is scalar, G_{ss} is independent of G_c, and thus (e), which shows the frequency response of G_{ss} for the controller (50), (51), is identical to (f), which shows the frequency response of G_{ss} for the controller (52), (53).

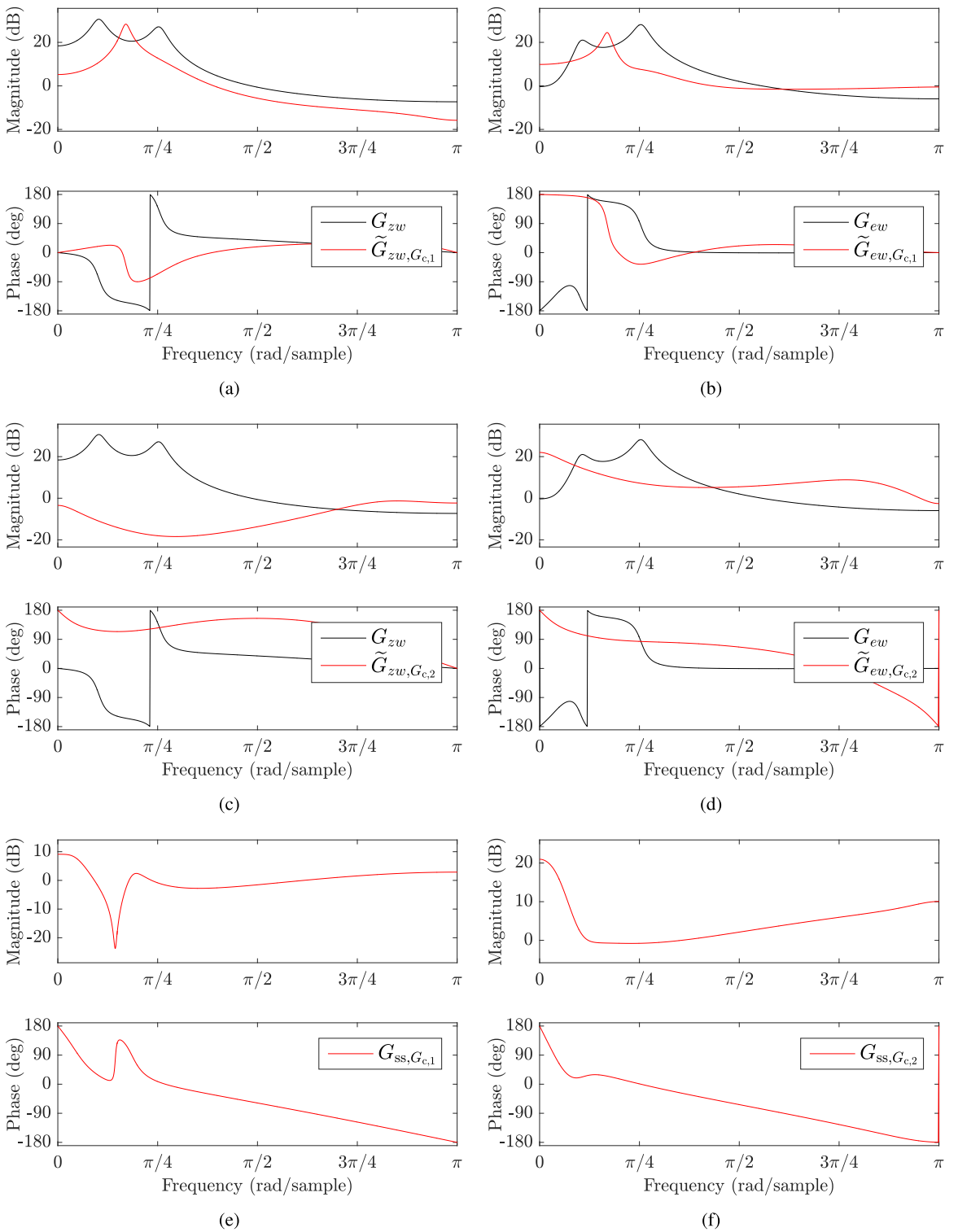

Fig. 7. Example 4: G_{ss} for feedback control with vector control $u \in \mathbb{R}^2$. (a) and (b) show the controlled and uncontrolled frequency response of the system (29), (30) using the controller (54), (55) denoted in the above legend as $G_{c,1}$; (c) and (d) show the controlled and uncontrolled frequency response of the system (29), (30) using the controller (56), (57) denoted in the above legend as $G_{c,2}$. Note that, since u is a vector, G_{ss} depends on G_c, and thus (e), which shows the frequency response of G_{ss} for the controller (54), (55), differs from (f), which shows the frequency response of G_{ss} for the controller (56), (57).

where

$$\widetilde{G}_{zw} \triangleq \frac{G_{zw}}{1 - G_{zu}G_{\mathrm{c}}}. \tag{39}$$

In addition, it follows from (36), (37), and (38) that

$$e = \widetilde{G}_{ew}w, \tag{40}$$

where

$$\widetilde{G}_{ew} \triangleq G_{eu}G_{\mathrm{c}}\widetilde{G}_{zw} + G_{ew} = \frac{G_{eu}G_{\mathrm{c}}G_{zw}}{1 - G_{zu}G_{\mathrm{c}}} + G_{ew}. \tag{41}$$

For feedback control, we define the spatial spillover function G_{ss} by

$$G_{\mathrm{ss}} \triangleq \frac{\dfrac{\widetilde{G}_{ew}}{G_{ew}} - 1}{\dfrac{\widetilde{G}_{zw}}{G_{zw}} - 1}, \tag{42}$$

which is identical in form to G_{ss} defined by (8) for feedforward control. As in the case of feedforward control, we assume that $G_{zu}G_{\mathrm{c}} \neq 0$. However, $\widetilde{G}_{zw}$ and $\widetilde{G}_{ew}$ defined by (39) and (41) for feedback control are different from $\widetilde{G}_{zw}$ and $\widetilde{G}_{ew}$ defined by (6) and (7) for feedforward control. It follows from (39) and (41) that

$$\frac{\widetilde{G}_{zw}}{G_{zw}} - 1 = \frac{G_{zu}G_{\mathrm{c}}}{1 - G_{zu}G_{\mathrm{c}}}, \tag{43}$$

$$\frac{\widetilde{G}_{ew}}{G_{ew}} - 1 = \frac{G_{eu}G_{\mathrm{c}}G_{zw}}{G_{ew}(1 - G_{zu}G_{\mathrm{c}})}. \tag{44}$$

Therefore, (42) implies that

$$G_{\mathrm{ss}} = \frac{\dfrac{G_{eu}G_{\mathrm{c}}G_{zw}}{G_{ew}(1 - G_{zu}G_{\mathrm{c}})}}{\dfrac{G_{zu}G_{\mathrm{c}}}{1 - G_{zu}G_{\mathrm{c}}}} = \frac{G_{eu}G_{\mathrm{c}}G_{zw}}{G_{zu}G_{\mathrm{c}}G_{ew}}. \tag{45}$$

Note that (45) has the same form as G_{ss} given by (11) for feedforward control. In the case where u is scalar, it follows that

$$G_{\mathrm{ss}} = \frac{G_{eu}G_{zw}}{G_{zu}G_{ew}}, \tag{46}$$

which is independent of G_{c} and coincides with (12) for feedforward control.

5. Feedback control numerical examples

Consider a discrete-time state-space representation of the system (35), (36) given by (13)–(19) and the state-space representation of the feedback controller (37) given by

$$x_{\mathrm{c}}(k+1) = A_{\mathrm{c}}x_{\mathrm{c}}(k) + B_{\mathrm{c}}z(k), \tag{47}$$

$$u(k) = C_{\mathrm{c}}x_{\mathrm{c}}(k) + D_{\mathrm{c}}z(k), \tag{48}$$

where

$$G_{\mathrm{c}}(\mathbf{z}) = C_{\mathrm{c}}(\mathbf{z}I - A_{\mathrm{c}})^{-1}B_{\mathrm{c}} + D_{\mathrm{c}}. \tag{49}$$

In the subsequent feedback numerical examples, we consider the same plants as in the feedforward numerical examples section. We assume that w is zero-mean Gaussian white noise with standard deviation 1. Feedback controllers are designed to suppress the effect of w at z. No considerations are made in the controller design to suppress the effect of w at e. The details of the controller design are omitted since they are not relevant to the analysis.

In each example we compare the spatial spillover function for two different feedback controller designs applied to the same system. The spatial spillover function is computed using (42) which is a function of G_{zw}, G_{ew}, $\widetilde{G}_{zw}$ given by (39), and $\widetilde{G}_{ew}$ given by (41). We demonstrate that, if $l_u = 1$, then (42) is independent of G_{c}, whereas if $l_u > 1$, then (42) is not independent of G_{c}.

Example 3. G_{ss} for feedback control with scalar control u. Consider the system (23), (24) with scalar control u. We apply two different feedback controllers to this system, namely,

$$A_c = \begin{bmatrix} -1.02 & 0 & 0 & 0 \\ 0 & 0.44 & 0.66 & 0 \\ 0 & -0.66 & 0.44 & 0 \\ 0 & 0 & 0 & 0.47 \end{bmatrix}, \quad B_c = \begin{bmatrix} 0.49 \\ 0.42 \\ 1.08 \\ 1.12 \end{bmatrix}, \tag{50}$$

$$C_c = \begin{bmatrix} -0.97 & 0.17 & 0.02 & 0.10 \end{bmatrix}, \quad D_c = 0 \tag{51}$$

and

$$A_c = \begin{bmatrix} -1.35 & 0 & 0 & 0 & 0 \\ 0 & 0.60 & 0.65 & 0 & 0 \\ 0 & -0.65 & 0.60 & 0 & 0 \\ 0 & 0 & 0 & 0.58 & 0 \\ 0 & 0 & 0 & 0 & -0.34 \end{bmatrix}, \quad B_c = \begin{bmatrix} -0.87 \\ 1 \\ -1.72 \\ -1.46 \\ -0.54 \end{bmatrix}, \tag{52}$$

$$C_c = \begin{bmatrix} 0.84 & -0.17 & -0.13 & -0.09 & -0.04 \end{bmatrix}, \quad D_c = 0. \tag{53}$$

For both controllers, Fig. 6 shows the frequency response of the controlled and uncontrolled system at z and e as well as the frequency response of G_{ss}. Since u is scalar, G_{ss} is the same for both controllers.

Example 4. G_{ss} *for feedback control with vector control* u. Consider the system (29), (30), where $u \in \mathbb{R}^2$. We apply two different feedback controllers to this system, namely,

$$A_c = \begin{bmatrix} -1.35 & 0 & 0 \\ 0 & -0.01 & 0.34 \\ 0 & -0.34 & -0.01 \end{bmatrix}, \quad B_c = \begin{bmatrix} -1.49 \\ 0.78 \\ -2.16 \end{bmatrix}, \tag{54}$$

$$C_c = \begin{bmatrix} -0.62 & 0.61 & 0.47 \\ -0.58 & -0.56 & 0.20 \end{bmatrix}, \quad D_c = \begin{bmatrix} 0 \\ 0 \end{bmatrix} \tag{55}$$

and

$$A_c = \begin{bmatrix} -1.96 & 0 & 0 & 0 \\ 0 & 0.38 & 0.37 & 0 \\ 0 & -0.37 & 0.38 & 0 \\ 0 & 0 & 0 & 0.16 \end{bmatrix}, \quad B_c = \begin{bmatrix} -1.98 \\ 4.27 \\ -4.60 \\ 4.26 \end{bmatrix}, \tag{56}$$

$$C_c = \begin{bmatrix} -0.46 & 0.18 & -0.29 & -0.70 \\ -0.75 & 0.74 & -1.26 & 0.05 \end{bmatrix}, \quad D_c = \begin{bmatrix} 0 \\ 0 \end{bmatrix}. \tag{57}$$

For both controllers, Fig. 7 shows the frequency response of the controlled and uncontrolled system at z and e as well as the frequency response of G_{ss}. Note that, since u is a vector, G_{ss} depends on G_c.

6. Spatial spillover as a ratio of transmissibilities

Consider the case where z, e, w, and u are scalar signals and introduce the notation

$$G_{zw} = \frac{N_{zw}}{D_{zw}} \quad G_{ew} = \frac{N_{ew}}{D_{ew}} \quad G_{zu} = \frac{N_{zu}}{D_{zu}} \quad G_{eu} = \frac{N_{eu}}{D_{eu}} \tag{58}$$

Assume that $D_{zw} = D_{ew}$ and $D_{zu} = D_{eu}$. The transmissibility [8–10] from z to e driven by w is given by

$$T_{ez,w} \triangleq \frac{G_{ew}}{G_{zw}} = \frac{\frac{N_{ew}}{D_{ew}}}{\frac{N_{zw}}{D_{zw}}} = \frac{N_{ew}}{N_{zw}}. \tag{59}$$

Similarly, the transmissibility from z to e driven by u is given by

$$T_{ez,u} \triangleq \frac{G_{eu}}{G_{zu}} = \frac{N_{eu}}{N_{zu}}. \tag{60}$$

Therefore, it follows from (12) and (46) that

$$G_{ss} = \frac{G_{eu}G_{zw}}{G_{zu}G_{ew}} = \frac{N_{eu}N_{zw}}{N_{zu}N_{ew}} = \frac{\frac{N_{eu}}{N_{zu}}}{\frac{N_{ew}}{N_{zw}}} = \frac{T_{ez,u}}{T_{ez,w}}. \tag{61}$$

Hence G_{ss} can be expressed as the ratio of two transmissibility functions.

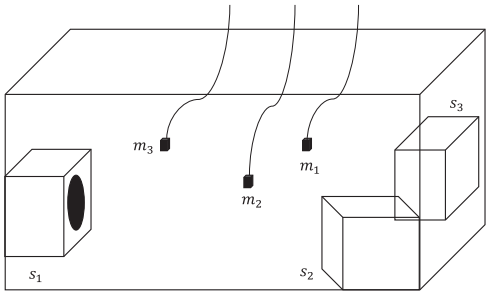

Fig. 8. Sensor and actuator placement.

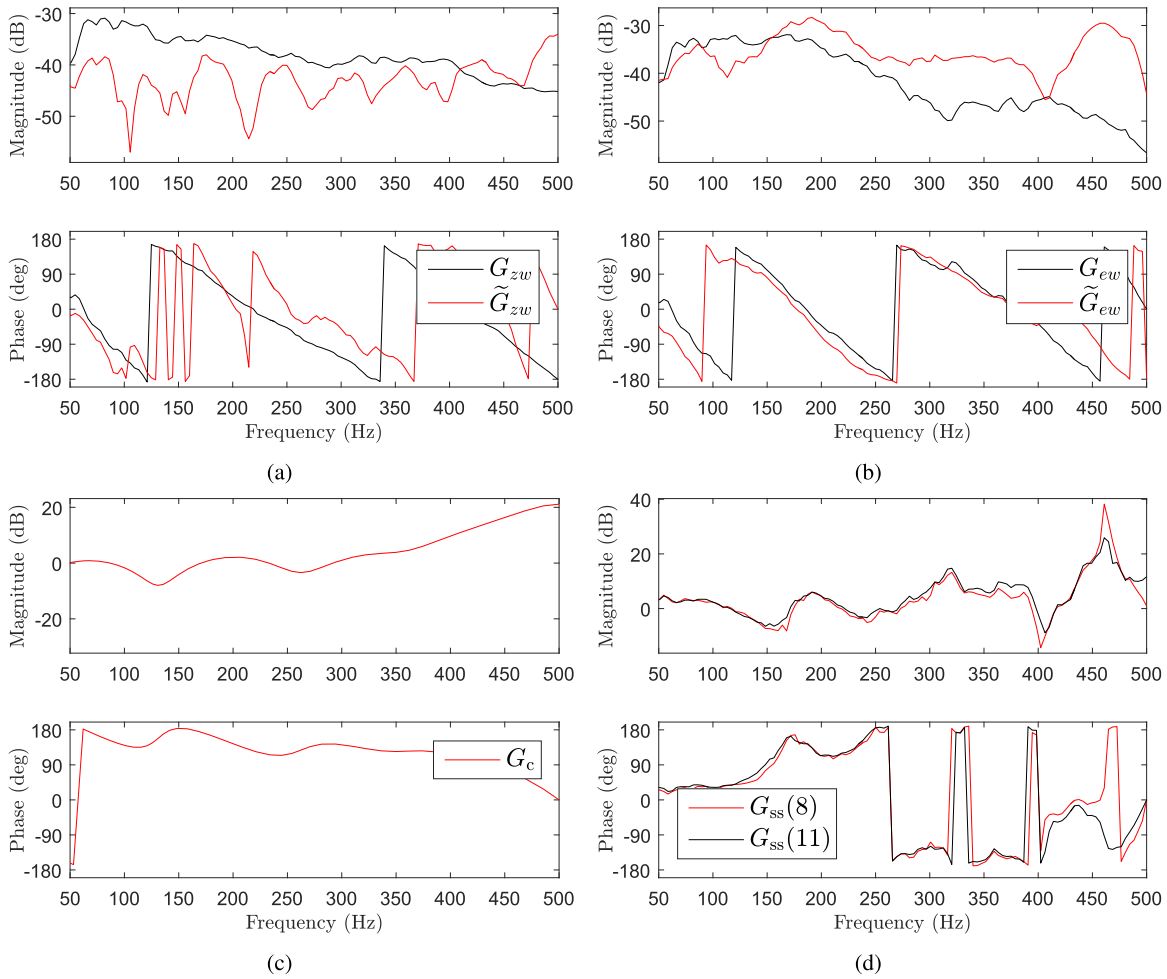

Fig. 9. Example 5: comparison of G_{ss} for feedforward control with scalar control u. (a) and (b) show the controlled and uncontrolled frequency response at z and e; (c) shows the frequency response of the controller. (d) compares G_{ss} estimated using (8) and (11).

7. Experimental results

7.1. Experimental setup

We apply feedforward and feedback controllers to an acoustic experiment to investigate the spatial spillover function. Omni-directional microphones are used as sensors, and mid-bass woofers are used as the actuation. Real Time Workshop (RTW) and MATLAB/Simulink is used with a dSPACE DS1104 board to implement the designed controllers. Additional hardware used in implementation included speaker amplifiers, microphone amplifiers, and anti-aliasing filters. A diagram of the microphone and speaker placement is shown in Fig. 8. The approximate dimensions of the acoustic space are 6 ft×3 ft×3 ft. We consider three microphone locations m_1, m_2, and m_3, and three speaker locations s_1, s_2, and s_3. In the subsequent experiments, one microphone is chosen as the performance microphone z, a separate microphone is chosen as the evaluation microphone e, one speaker is chosen to produce a disturbance w, and either one or both of the remaining speakers are chosen as the control speaker u. The frequency range of interest for this study is from 50 Hz to 500 Hz, with all data sampled at 1 kHz. Each data set is ran for 10,000 samples and multiple runs are repeated to check for consistency. In all experimental examples, the disturbance w is chosen as zero-mean Gaussian white noise.

7.2. Experimental determination and validation of the spatial spillover function

In the subsequent feedforward control experiments, two methods for estimating the spatial spillover function G_{ss} are compared. We estimate G_{ss} using both (8) and (11). The Blackman-Tukey spectral analysis method [11] with a Hanning window is applied to input-output data in order to estimate the frequency response of various transfer functions in G_{ss}.

Determining G_{ss} using (8) requires estimates of G_{zw}, G_{ew}, $\widetilde{G}_{zw}$, and $\widetilde{G}_{ew}$. The frequency response of G_{zw} and G_{ew} are

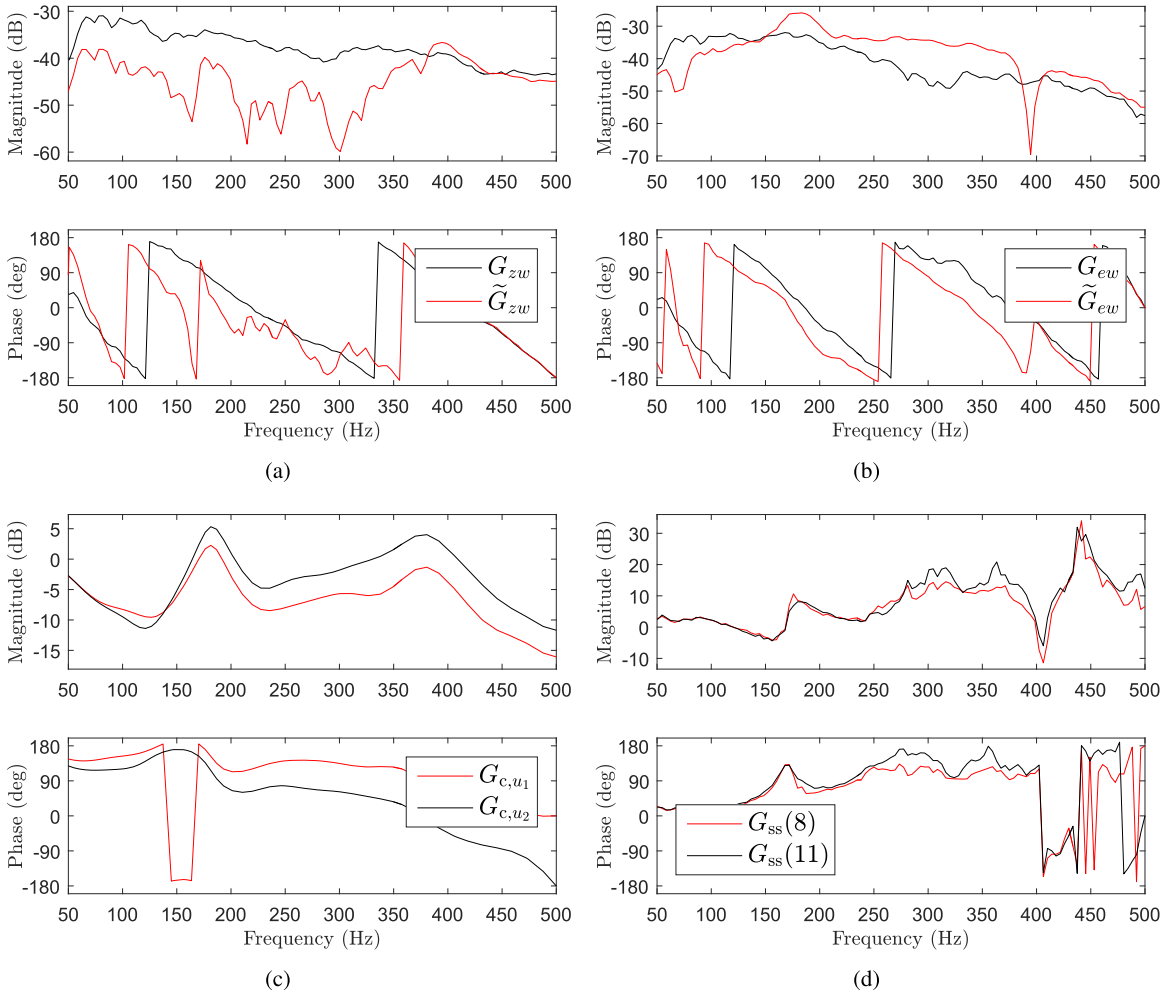

Fig. 10. Example 6: comparison of G_{ss} for feedforward control with vector control $u \in \mathbb{R}^2$. (a) and (b) show the controlled and uncontrolled frequency response at z and e; (c) shows the frequency response of both channels the controller. (d) compares G_{ss} estimated using (8) and (11).

estimated by exciting the system with a known broadband input w and sampling the z microphone and e microphone outputs. The frequency response of $\widetilde{G}_{zw}$ and $\widetilde{G}_{ew}$ are estimated by applying the controller to the system with a known disturbance w and similarly obtaining measurements of the output signals z and e. Determining G_{ss} using (11) requires estimates of G_{zw}, G_{ew}, G_{zu}, and G_{eu}, and, in the case where u is a vector, depends on the design of G_c. The frequency response of G_{zw} and G_{ew} are estimated as described above. The frequency response of G_{zu} and G_{eu} are estimated by exciting the system with a known broadband input u and sampling the z microphone and e microphone outputs.

Note that G_{ss} estimated as (8) requires applying the controller to the system, whereas G_{ss} estimated as (11) does not. The goal of the experimental examples is to show that the estimated frequency response of (8) and (11) agree, despite the fact that one method requires applying the controller to the system. In practice, it may be more advantageous to estimate G_{ss} as (11) since the identification of G_{zu} and G_{eu} is of lower order and the expression is less complex than $\widetilde{G}_{zw}$ and $\widetilde{G}_{ew}$. Similar logic applies to the feedback case between estimating G_{ss} as (42) and (45). The details of the controller design are again omitted since they are not relevant to the analysis of G_{ss}. We note that in all experimental examples, the matching between G_{ss} estimated using the two methods degrades as the Nyquist rate is approached. Furthermore, it was observed that if $\frac{\widetilde{G}_{ew}}{G_{ew}} \approx 1$, the matching between the two methods can be adversely effected.

7.2.1. Experimental results using feedforward control

Example 5. Comparison of G_{ss} for feedforward control with scalar control u. We choose m_2 as z, m_1 as e, s_1 as w, and s_2 as u. A feedforward controller is designed to suppress the effect of w at z. Fig. 9 shows the frequency response of the controller, the controlled and uncontrolled system at z and e, and G_{ss} estimated using (8) and (11). The magnitude and phase of G_{ss} estimated using (8) and (11) are within 5 dB and 10° from 50 Hz to 380 Hz, and within 12 dB and 60o from 250 Hz to 500 Hz.

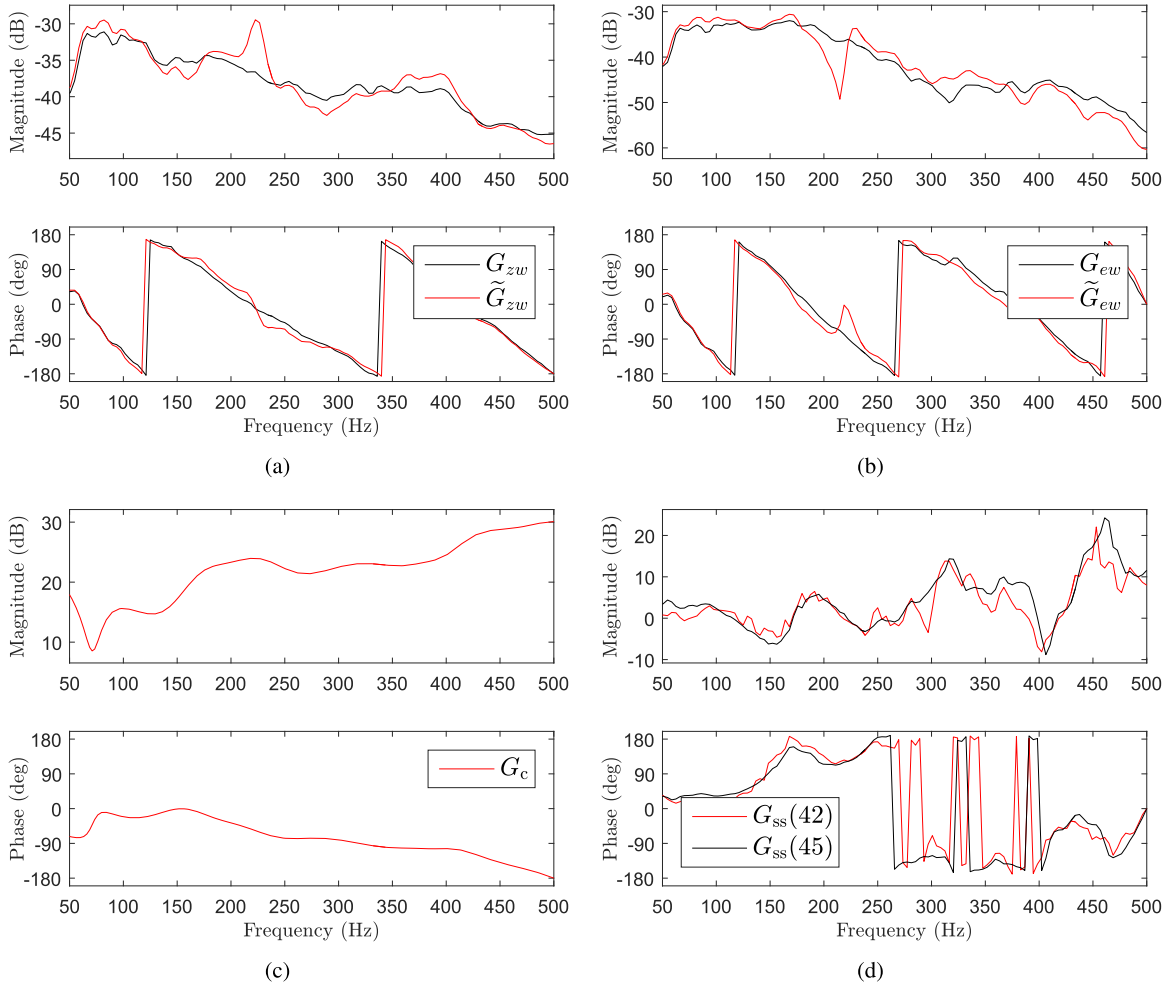

Fig. 11. Example 7: comparison of G_{ss} for feedback control with scalar control u. (a) and (b) show the controlled and uncontrolled frequency response at z and e; (c) shows the frequency response of the controller. (d) compares G_{ss} estimated using (42) and (45).

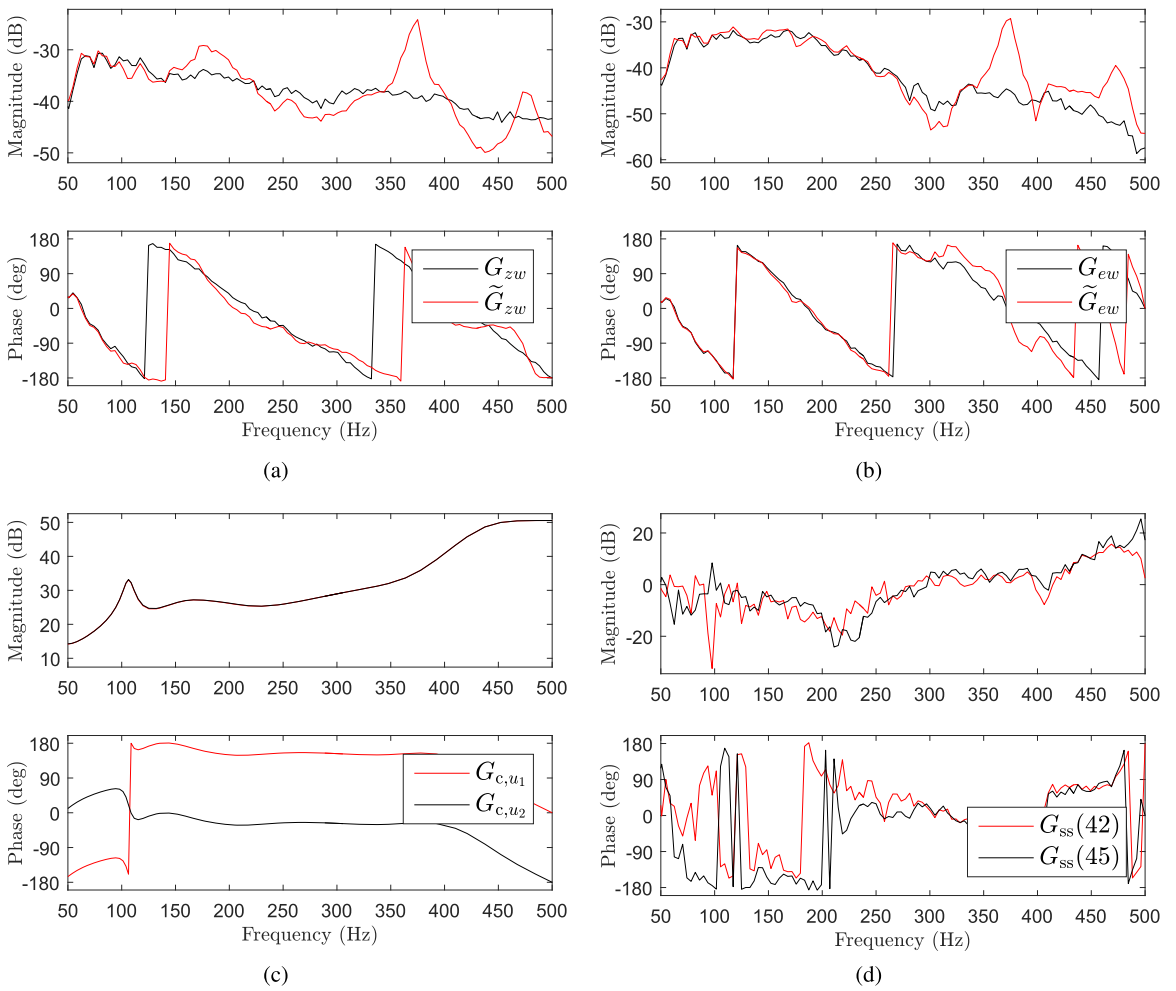

Fig. 12. Example 8: comparison of G_{ss} for feedback control with vector control $u \in \mathbb{R}^2$. (a) and (b) show the controlled and uncontrolled frequency response at z and e; (c) shows the frequency response of both channels the controller. (d) compares G_{ss} estimated using (42) and (45).

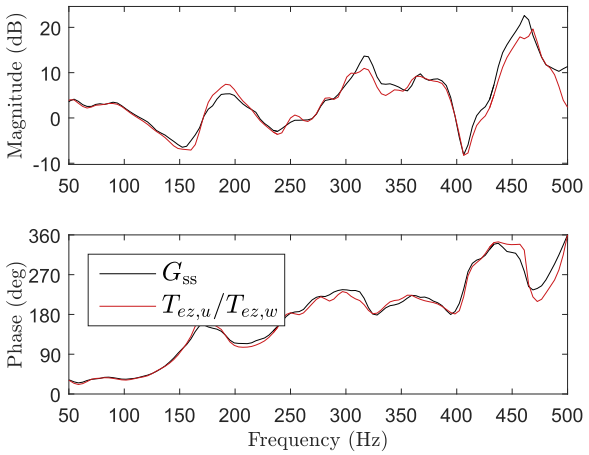

Fig. 13. Example 9: comparison of G_{ss} for scalar control u, estimated as (12), shown in black, and (61), shown in red. (For interpretation of the references to color in this figure legend, the reader is referred to the web version of this article.)

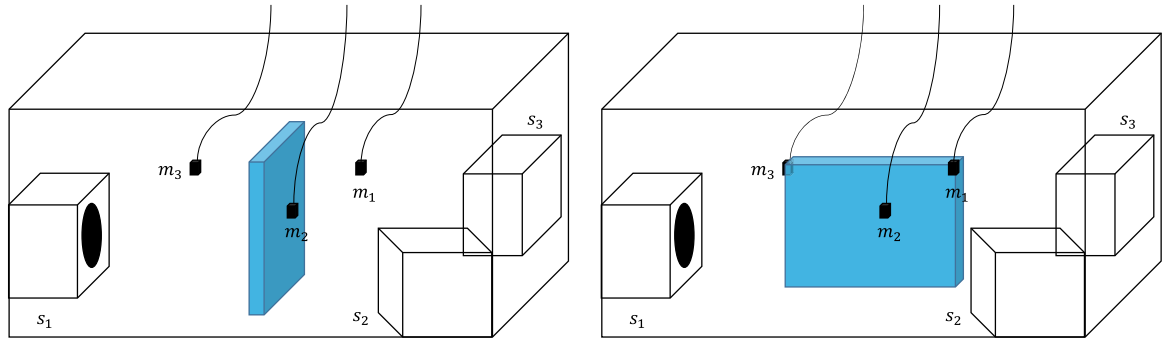

Fig. 14. Diagram of two different obstructions tested in acoustic space. (a) shows a height-wise obstruction, and (b) shows a length-wise obstruction.

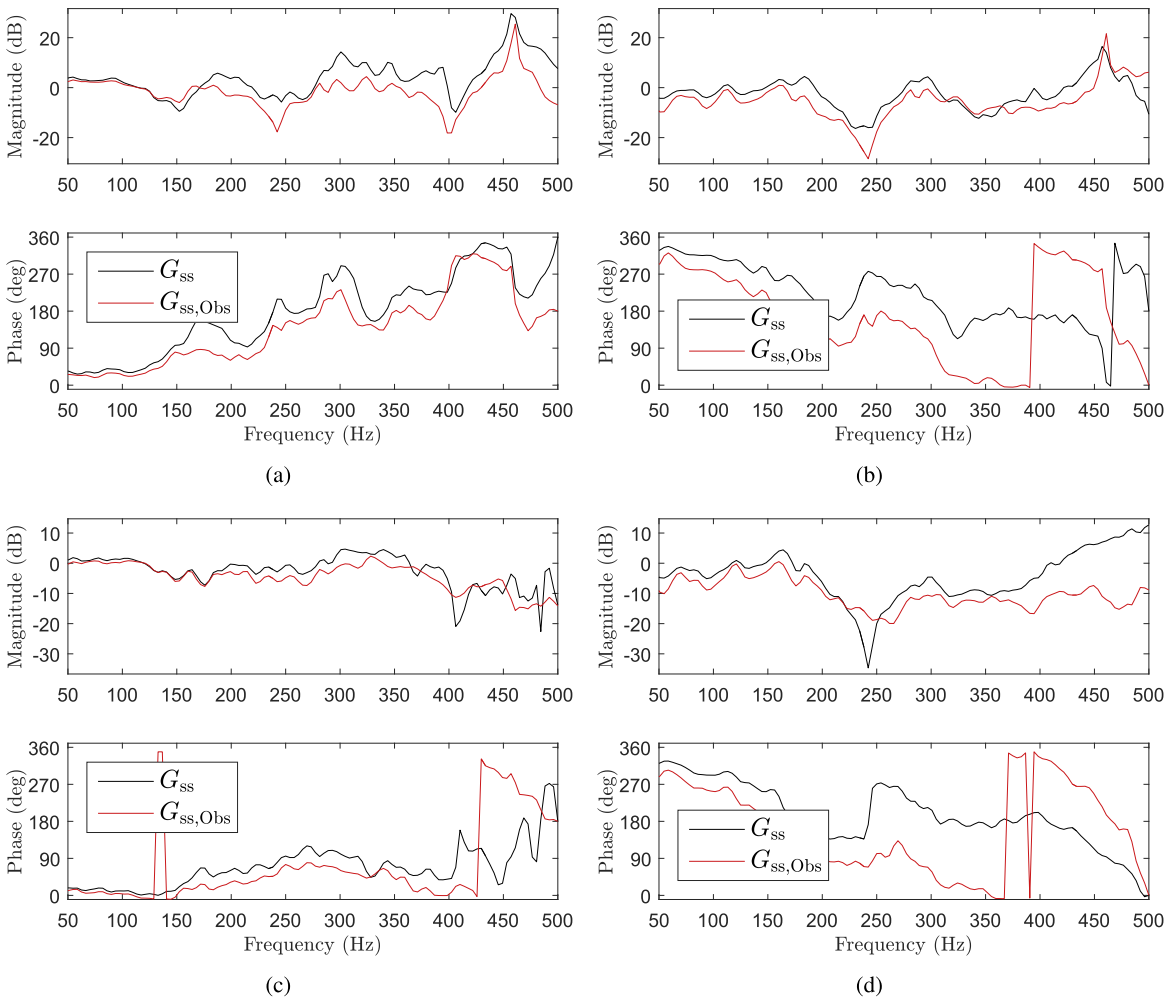

Fig. 15. Example 10: comparison of G_{ss} with and without a height-wise obstruction in the acoustic space. (a) shows G_{ss} for z and e_1 with s_3 as u, and (b) shows G_{ss} for z and e_2 with s_3 as u. Note that in (a), the magnitude and phase of G_{ss} noticeably shifts due to the obstruction. In (b), the magnitude of G_{ss} slightly shifts due to the obstruction while the phase of G_{ss} significantly shifts due to the obstruction. (c) shows G_{ss} for z and e_1 with s_1 as u, and (d) shows G_{ss} for z and e_2 with s_1 as u. Note that in (c), the magnitude and phase of G_{ss} slightly shifts due to the obstruction. In (d), the magnitude and phase of G_{ss} significantly shifts due to the obstruction.

Example 6. Comparison of G_{ss} for feedforward control with vector control $u \in \mathbb{R}^2$. We choose m_2 as z, m_1 as e, s_1 as w, s_2 as u_1, and s_3 as u_2. A feedforward controller is designed to suppress to suppress the effect of w at z. Fig. 10 shows the frequency response of the controller, the controlled and uncontrolled system at z and e, and G_{ss} estimated using (42) and (45). The magnitude and phase of G_{ss} estimated using (42) and (45) are within 5 dB and 10° from 50 Hz to 250 Hz, and within 12 dB and 60° from 250 Hz to 500 Hz.

7.2.2. *Experimental results using feedback control*

Example 7. Comparison of G_{ss} for feedback control with scalar control u. Consider the same choice of microphones and speakers as in Example 5. A feedback controller is designed to suppress the effect of w at z. Fig. 11 shows the frequency response of the controller, the controlled and uncontrolled system at z and e, and G_{ss} estimated using (42) and (45). The magnitude and phase of G_{ss} estimated using (42) and (45) are within 5 dB and 20° from 50 Hz to 250 Hz, and within 12 dB and 40° from 250 Hz to 500 Hz.

Example 8. Comparison of G_{ss} for feedback control with vector control $u \in \mathbb{R}^2$. Consider the same choice of microphones and speakers as in Example 6. A feedback controller is designed to suppress the effect of w at z. Fig. 12 shows the frequency response of the controller, the controlled and uncontrolled system at z and e, and G_{ss} estimated using (42) and (45). The magnitude and phase of G_{ss} estimated using (42) and (45) are mismatched from 50 Hz to 100 Hz, and from 200 Hz to 250 Hz, where the difference between the two estimates exceeds 15 dB and 60°. At other frequencies, the magnitude and phase are within 5 dB and 20°. The large mismatch is partially due to the fact that $\widetilde{G}_{ew} \approx G_{ew}$ across those bands, and thus the numerator of (42) becomes approximately zero causing the numerical accuracy of the estimate to degrade.

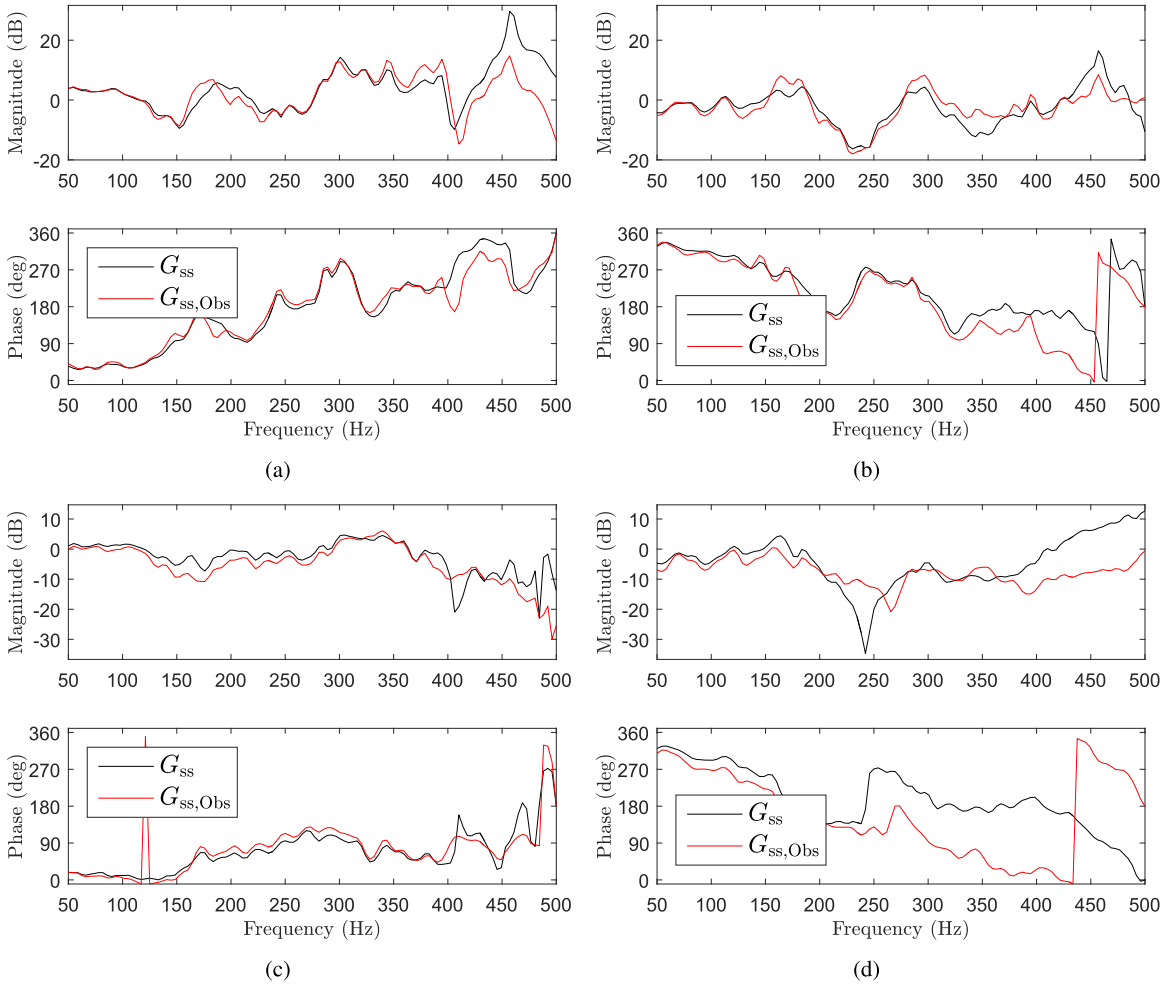

Fig. 16. Example 11: comparison of G_{ss} with and without a length-wise obstruction in the acoustic space. (a) shows G_{ss} for z and e_1 with s_3 as u, and (b) shows G_{ss} for z and e_2 with s_3 as u. Note that in both (a) and (b), the magnitude and phase of G_{ss} does not shift across the low and mid frequencies, but noticeably shifts at high frequencies due to the obstruction. (c) shows G_{ss} for z and e_1 with s_1 as u, and (d) shows G_{ss} for z and e_2 with s_1 as u. Note that in (c), the magnitude and phase of G_{ss} does not shift due to the obstruction. In (d), the magnitude and phase of G_{ss} significantly shifts due to the obstruction.

7.3. Computing G_{ss} as a ratio of transmissibilities

Consider the case where u is a scalar. G_{ss} can be estimated using (61), which is a ratio of transmissibility functions. The advantage of this method is that estimating the frequency response of a transmissibility function does not explicitly require the input to be known, but only needs measurements of the ouptut. Hence, if a measurement of disturbance w is unavailable, an estimate of G_{ss} is still obtainable using only measurements of z and e. The disadvantage of estimating G_{ss} using (61) is that the in order to estimate $T_{ez,u}$, the system must be excited only by u without the presence of w and vice versa when estimating $T_{ez,w}$. We compare G_{ss} estimated using (12) and (61), which are expected to agree.

Example 9. G_{ss} as a ratio of Transmissibilities. We choose m_1 as e, m_2 as z, s_1 as w, and s_3 as u. Fig. 13 compares the frequency response of G_{ss} estimated using (12) and (61). The magnitude and phase of G_{ss} estimated as (12) and (61) are within 5 dB and 20° from 50 Hz to 450 Hz, and within 9 dB and 50° from 450 Hz to 500 Hz.

7.4. G_{ss} in the presence of obstructions

We examine G_{ss} in the presence of obstructions by comparing the estimate of G_{ss} between sensors with and without the presence of an obstruction. In the subsequent examples, G_{ss} estimated as (12), where we assume u is a scalar, using methods described above. Fig. 14 shows a diagram of the two configurations considered in the acoustic space. In each example, one microphone is chosen as z, one speaker is chosen as w, two e locations, denoted as e_1 and e_2, are chosen, and two separate locations for u are considered. The spatial spillover function is estimated for the pair z and e_1 and the pair z and e_2 for both choices of u. In certain cases, the presence of obstruction can significantly shift the magnitude and phase of the spatial spillover function relative to when the obstruction is not present.

Example 10. Comparison of G_{ss} with and without a height-wise obstruction. We choose m_2 as z, s_1 as w, and two e locations, with m_1 as e_1 and m_3 as e_2. We consider two choices of u, where for the first system we choose s_3 as u, and the second system we choose s_2 as u. Comparison of G_{ss} with and without a height-wise obstruction in the acoustic space for both choices of u is shown in Fig. 15. Of the four cases considered in the example, a noticeable or significant shift in the magnitude and phase of G_{ss} is observed in three cases.

Example 11. Comparison of G_{ss} with and without a length-wise obstruction. We consider the same choices of speakers and microphones as in Example 10, and place a length-wise obstruction in the acoustic space. Comparison of G_{ss} with and without a length-wise obstruction in the acoustic space for both choices of u is shown in Fig. 16. Of the four cases considered in the example, a noticeable or significant shift in the magnitude and phase of G_{ss} is observed in one case.

8. Conclusions and future research

The spatial spillover function was validated in both numerical and experimental studies, and it was shown that the expression for G_{ss} is the same for both feedforward and feedback control. In the case where u is a scalar signal, the spatial spillover function is independent of the controller, and G_{ss} can be interpreted as a ratio of transmissibility functions. It was found that obstructions in the acoustic space may give rise to significant shifts in the magnitude and phase of G_{ss}. A systematic numerical study on the robustness of G_{ss} is left for future work. Finally, all the examples in this paper are carried out for a single, representative controller. The analysis of spatial spillover has implications for controller synthesis, and this will be considered in future work.

Acknowledgments

This research was supported in part by NSF Grant CMMI 1160916.

References

[1] C.R. Fuller, A.H. von Flotow, Active control of sound and vibration, *IEEE Control Syst. Mag.* 15 (6) (1995) 9–19, http://dx.doi.org/10.1109/37.476383.
[2] P.A. Nelson, S.J. Elliot, *Active Control of Sound*, Academic Press, San Diego, CA, USA, http://dx.doi.org/10.1049/ecej:19900032.
[3] S.M. Kuo, D.R. Morgan, *Active Noise Control Systems: Algorithms and DSP Implementations*, Wiley, New York, NY, USA, 1995.
[4] J.C. Doyle, B.A. Francis, A.R. Tannenbaum, *Feedback Control Theory*, Macmillan, New York, NY, USA, 1992.
[5] J. Hong, D.S. Bernstein, Bode integral constraints, colocation, and spillover in active noise and vibration control, *IEEE Trans. Control Syst. Technol.* 6 (1998) 111–120, http://dx.doi.org/10.1109/87.654881.
[6] J.S. Freudenberg, C.V. Hollot, R.H. Middleton, V. Toochinda, Fundamental design limitations of the general control configuration, *IEEE Trans. Autom. Control* 48 (2003) 1355–1370, http://dx.doi.org/10.1109/TAC.2003.815017.

[7] A. Xie, D. S. Bernstein, Experimental investigation of spatial spillover in adaptive noise control of broadband disturbances in a 3D acoustic space, in: Proceedings of the American Control Conference, Boston, MA, July 2016.
[8] N. Maia, A. Urgueira, R. Almeida, Whys and wherefores of transmissibility, in: F. Beltran-Carbajal (Ed.), *Vibration Analysis and Control*, 2011, pp. 197–216, http://dx.doi.org/10.1109/87.654881. (Chapter 10).
[9] C. Devriendt, P. Guillaume, Identification of modal parameters from transmissibility measurements, *J. Sound Vib.* 314 (2008) 343–356, http://dx.doi.org/10.1016/j.jsv.2007.12.022.
[10] K.F. Aljanaideh, D.S. Bernstein, Time-domain analysis of motion transmissibilities in force-driven and displacement-driven structures, *J. Sound Vib.* 347 (2015) 169–183, http://dx.doi.org/10.1016/j.jsv.2015.01.018.
[11] P. Stoica, R.L. Moses, *Introduction to Spectral Analysis*, Prentice Hall, Upper Saddle River, 1997.